Ann. Geophys., 35, 1269–1274, 2017
https://doi.org/10.5194/angeo-35-1269-2017

Annales Geophysicae Open Access EGU

Tail reconnection in the global magnetospheric context: Vlasiator first results

Minna Palmroth[1,2], Sanni Hoilijoki[1], Liisa Juusola[2], Tuija I. Pulkkinen[3], Heli Hietala[4], Yann Pfau-Kempf[1], Urs Ganse[1], Sebastian von Alfthan[5], Rami Vainio[6], and Michael Hesse[7]

[1]Department of Physics, University of Helsinki, Helsinki, Finland
[2]Earth Observation, Finnish Meteorological Institute, Helsinki, Finland
[3]School of Electrical Engineering, Aalto University, Espoo, Finland
[4]Institute of Geophysics and planetary physics, University of California, Los Angeles, USA
[5]CSC – IT Center for Science, Espoo, Finland
[6]Department of Physics and Astronomy, University of Turku, Turku, Finland
[7]Department of Physics and Technology, University of Bergen, Bergen, Norway

Correspondence to: Minna Palmroth (minna.palmroth@helsinki.fi)

Received: 31 July 2017 – Revised: 23 October 2017 – Accepted: 24 October 2017 – Published: 28 November 2017

Abstract. The key dynamics of the magnetotail have been researched for decades and have been associated with either three-dimensional (3-D) plasma instabilities and/or magnetic reconnection. We apply a global hybrid-Vlasov code, Vlasiator, to simulate reconnection self-consistently in the ion kinetic scales in the noon–midnight meridional plane, including both dayside and nightside reconnection regions within the same simulation box. Our simulation represents a numerical experiment, which turns off the 3-D instabilities but models ion-scale reconnection physically accurately in 2-D. We demonstrate that many known tail dynamics are present in the simulation without a full description of 3-D instabilities or without the detailed description of the electrons. While multiple reconnection sites can coexist in the plasma sheet, one reconnection point can start a global reconfiguration process, in which magnetic field lines become detached and a plasmoid is released. As the simulation run features temporally steady solar wind input, this global reconfiguration is not associated with sudden changes in the solar wind. Further, we show that lobe density variations originating from dayside reconnection may play an important role in stabilising tail reconnection.

Keywords. Magnetospheric physics (magnetotail; plasma sheet) – space plasma physics (magnetic reconnection)

1 Introduction

Magnetic reconnection is the central process in driving Earth's magnetospheric dynamics, since it transfers energy from the solar wind into the magnetosphere (e.g. Dungey, 1961; Palmroth et al., 2006; Pulkkinen et al., 2010). Modelling of space plasmas is important not only as context to data but also to develop prediction capabilities needed to understand societal consequences of space weather (e.g. Watermann et al., 2009). So far, the global reconnection process including both the dayside and nightside reconnection regions has been modelled mostly with global magnetohydrodynamic (MHD) codes (e.g. Laitinen et al., 2005; Wiltberger et al., 2015). More sophisticated plasma descriptions, like the fully and partially kinetic approaches, have been applied in local geometries (e.g. Zeiler et al., 2002; Lapenta et al., 2015) and also recently in global setups (Lin et al., 2014, 2017; Lu et al., 2015). In the local simulations studying tail reconnection, tail reconnection needs to be initiated artificially by an additional perturbation, which may not correctly represent the driving of tail reconnection by reconnected magnetic flux from the dayside.

In this paper, we present the first global hybrid-Vlasov simulation of the magnetosphere, including both dayside and nightside reconnection regions in the same self-consistent simulation box. This allows us to study tail reconnection as a function of driving by dayside reconnection, which, regardless of steady solar wind, can vary (Hoilijoki et al., 2017). We

AnGeo Communicates

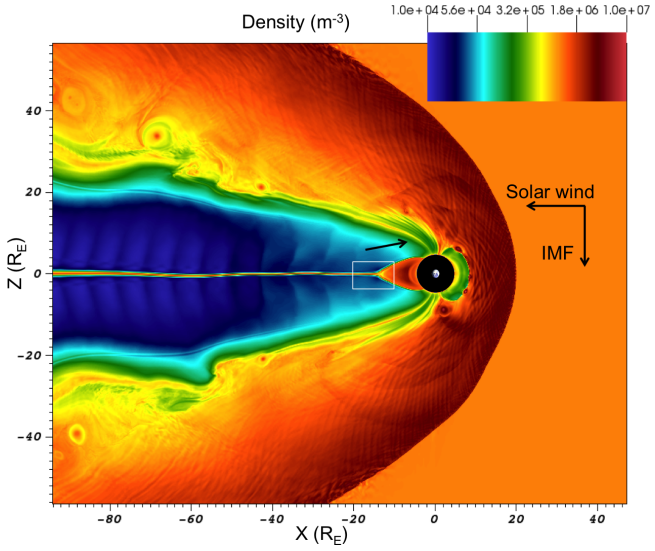

Figure 1. The plasma density in the Earth's magnetosphere as depicted by the Vlasiator simulation in the geocentric solar ecliptic (GSE) coordinate system used in this paper. Figure 1 is a snapshot of Supplement movie S1 showing the entire simulation sequence in time. The white rectangle in the tail shows the zooming area in Fig. 2 and in Supplement movie S2. The arrow inside the magnetopause is discussed later in connection to Fig. 4.

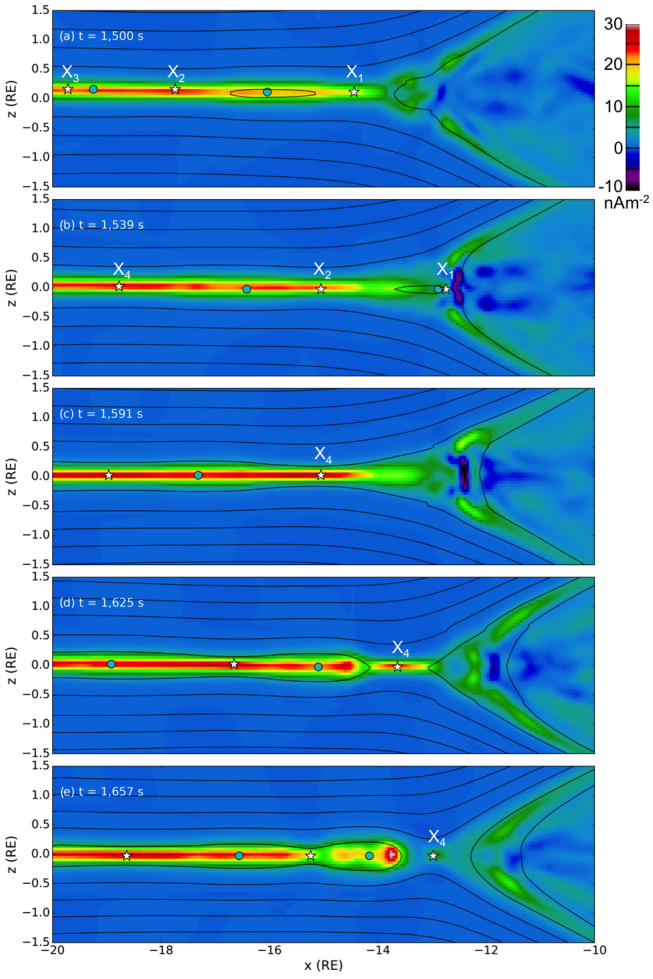

Figure 2. Zoom to the tail plasma sheet, with current density colour-coded, showing the duskward current component flowing in the tail plasma sheet in the $X-Z$ plane. Reconnection locations are marked with white stars, while magnetic islands are cyan circles. Some reconnection locations are identified with X_n, $(n = 1\ldots4)$, and panels **(a)**–**(e)** show their evolution in time.

first present the run overview, after which we investigate tail reconnection in more detail. In particular, we observe that reconnection can either occur locally within the plasma sheet, or it can spread to involve lobe field lines and build a major reconnection (X) point. We concentrate on two major X-point events and suggest that a lobe flux tube filled by bursts of dayside reconnection may have a role in building one of these events.

2 Vlasiator

Vlasiator (Palmroth et al., 2013, 2015; von Alfthan et al., 2014) describes protons by a full six-dimensional (6-D) velocity distribution, while electrons are a charge-neutralising fluid. This approach neglects electron kinetic effects, but includes ion kinetic effects, allowing the modelling of the reconnection field geometry self-consistently as determined by ions and assuming that electrons do not affect the field configuration. The hybrid-Vlasov approach is similar to the hybrid-PIC (particle-in-cell) approach in that both include ion kinetic effects, while it differs from the PIC in that the distribution function is solved rather than constructed from particle statistics, ensuring noiseless simulation results. Furthermore, so far the majority of the hybrid-PIC results have been obtained with downscaled geomagnetic dipole strength. Vlasiator does not scale down the dipole strength, nor does it use scaled spatial or temporal units, making the temporal and spatial scales as well as time differences between the different parts of the model directly comparable with observations.

While Vlasiator supports full 6-D simulations that can be performed when computational resources allow, here we present a 5-D setup and a 2-D run in the polar plane, including a 3-D velocity space within each ordinary space cell. Using a 3-D full PIC simulation including both electrons and ions, Zeiler et al. (2002) shows that magnetic reconnection in the 3-D system remains nearly two-dimensional if the reconnection guide field is 0. Reconnection at a single X line will be nearly 2-D if there is no guide field. Typical tail reconnection events do not have a guide field (e.g. Eastwood et al., 2010), and at the subsolar dayside during purely southward interplanetary magnetic field (IMF), the guide field is 0. Further, as Vlasiator has been shown to reproduce the theoretical predictions of dayside reconnection rates with good

accuracy (Hoilijoki et al., 2017), we argue that there is sufficient grounds to address ion-scale reconnection in this 2-D simulation run.

Figure 1 and Supplement movie S1 show an overview of the run. Solar wind flows into the simulation box from the sunward wall. Other walls of the simulation box apply Neumann conditions, meaning that each parameter at the boundary is copied to the neighbouring ghost cell. The out-of-plane direction applies periodic boundary conditions. The simulation box extends from 48 R_E in the dayside to -94 R_E in the nightside and ± 56 R_E in the Z direction. The initial conditions for the calculations are the Earth's dipole strength, described as in Daldorff et al. (2014), and solar wind parameters, with a Maxwellian form for the solar wind population. The run features steady southward IMF of -5 nT. The density of the solar wind is 1 cm^{-3}. The solar wind velocity is -750 km s^{-1} along the x axis. The inner boundary of the simulation domain in this run is located at 5 R_E, and it is approximated as perfectly conducting.

The resolution in this run is 300 km in the ordinary space and 30 km s^{-1} in the velocity space throughout the simulation box. This resolution takes the ion-scale turbulence, for example, into account self-consistently. For reference, to our knowledge the only other global hybrid-PIC simulation that has investigated tail dynamics in detail used a resolution of 0.15 R_E (Lu et al., 2015; Lin et al., 2017), which is over 3-fold in comparison to the resolution presented here, making the resolution here unprecedented.

3 Reconnection in the global magnetosphere

Figure 2 shows a zoom of the cross-tail current J_Y in the plasma sheet. Supplement movie S2 shows this same zoom region with three parameters, current density, X component of the plasma velocity V_X, and the magnetic flux function Ψ calculated from $\boldsymbol{B} = \boldsymbol{y} \times \nabla\Psi$, where $\boldsymbol{B}$ is the in-plane magnetic field and $\boldsymbol{y}$ a unit vector in the out-of-plane direction. Magnetic reconnection locations and magnetic islands are identified by finding the local saddle points and maxima of the magnetic flux function, respectively (Yeates and Hornig, 2011; Hoilijoki et al., 2017). This method is robust and accurately describes reconnection when magnetic flux is moving with respect to the reconnection point. At simulation time $t = 150$ s, three X points are identified with labels X_1 to X_3. As time progresses, the ambient earthward plasma flow carries the X points towards the transition region between dipolar and stretched magnetic field lines. At time $t = 1539$ s, X_3 ceases to reconnect. Consequently X_2 and X_4 are left at a longer distance from each other.

At $t = 1591$ s, the trailing islands of both X_1 and X_2 have merged with the dipolar field in the transition region leading to their "annihilation", leaving X_4 as the closest X point to the transition region. When X_4 arrives at the transition region, its tailward island neighbour is still far away, allowing

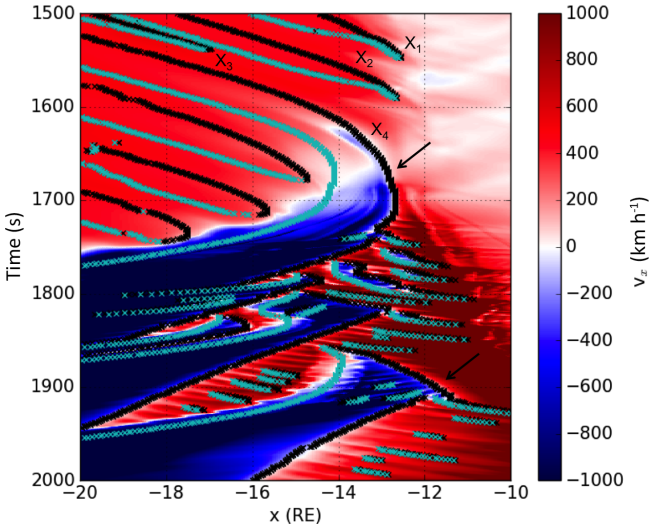

Figure 3. Motion of the X and O points in the tail. The background colour-coding shows the tail V_X as a function of time (on y axis, running from top to bottom to ease comparison with Fig. 2) and X location (in x axis) in the central plasma sheet. Individual X points are given as a function of time as black marks, while the magnetic islands are shown as cyan marks. X points X_1 to X_4 are labelled. The building of the two major X lines discussed in this paper are marked with an arrow.

X_4 to continue reconnecting. A thin current sheet starts to form around X_4 already at $t = 1607$ s and is best visible at $t = 1625$ s. The plasma transported tailwards by X_4 starts to divert around the trailing island, strengthening the southward magnetic field at the earthward edge of the island, separating the thin current sheet from the main plasma sheet. At $t = 1657$ s the separate thin current sheet has almost completely disrupted, and X_4 starts to process open lobe field lines. As soon as X_4 proceeds to reconnect open field lines, a global phase transition occurs and the tailward magnetic island as well as everything tailward of it is disconnected from the rest of the magnetotail and this plasmoid is swept downtail.

To investigate why X_4 starts the global change, Fig. 3 shows the locations of the X points as black marks and magnetic islands as cyan marks as a function of time. The background colour shows V_X in the plasma sheet. X_4 differs from its predecessors by the fact that it is located further away from surrounding X points, and therefore it does not experience as much pressure from neighbouring outflow regions (not shown). The tailward outflow from X_4 is strong enough to resist the trailing magnetic island, and the collision leading to X_4 annihilation is avoided. Figure 3 shows that there are three such occasions in the tail, when a major X point builds up to divert plasma flow within the plasma sheet. All three are also associated with plasmoid releases.

Figure 3 and movie S2 show that after $t \sim 1710$ s, the X point closest to the Earth starts to burst plasma tailward and

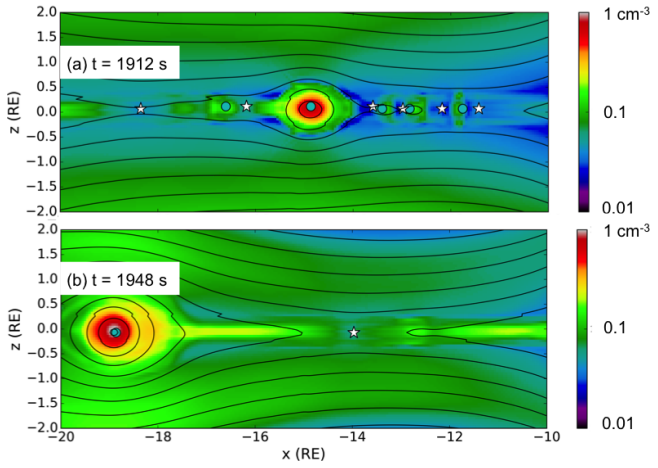

Figure 4. Plasma density in a zoomed area in the tail for **(a)** $t =$ 1912 s and **(b)** $t = 1948$ s. X points and magnetic islands are marked as in Fig. 2.

earthward. The fast outflow speeds lead to distorted field lines, leading to new X points (e.g. $t = 1804$ s), adding to the flow bursts. At about $t \sim 1920$ s a flux tube of higher density, filled by bursts of dayside magnetopause reconnection, sinks into the plasma sheet. This "stripe" of denser plasma is visible already in Fig. 1 just inside the magnetopause (marked by an arrow), and its motion is depicted in the movie S1. Figure 4 shows the influence of the higher-density flux tube in more detail. Before the higher density reaches the central plasma sheet, multiple X-point reconnections occur, while after the higher density arrives, a single stable X point is formed. As the reconnection outflow speed is given by the Alfvén speed of the inflowing plasma, higher density in the inflow region leads to a decrease in the outflow speeds. The slower outflow suppresses multiple reconnection points, for which we suggest the following mechanism: a new X point needs distorted field geometries. Large outflow speeds lead to bursty outflows, which favour new X points due to varying field geometries associated with the bursts. The decreased outflow speeds suppress the flow bursts, leading to smoother field geometries as can be seen from movie S2. With smoother field geometries, the conditions are not favourable to new multiple X points, leading to once more a dominant stable X point.

4 Discussion and conclusions

We carried out an ion-scale simulation of the global magnetosphere in 5-D with Vlasiator. The kinetic-scale system is driven by solar wind and IMF, which lead to dayside reconnection and open flux generation, transferring to the nightside to drive tail reconnection. Our results indicate that first multiple reconnection points operate simultaneously, interacting with each other, after which (at $t = 1657$ s) a major X point forms when reconnection starts to process the lobe field lines. The formation of the major X point by processing of lobe field lines has already been described with a 2-D MHD simulation (Lyon et al., 1981). Using a local two-fluid simulation of the current sheet, Ohtani et al. (2004) shows multiple X points, of which one starts to dominate after reconnection spreads to the lobe field lines. Similar conclusions are made based on local kinetic simulations (Lapenta et al., 2015) and by global hybrid-PIC simulations (Lin et al., 2014). The earthward-moving multiple reconnection sites have been observed by, e.g., Eastwood et al. (2005) using the Cluster spacecraft. We confirm that the global hybrid-Vlasov approach also reproduces multiple X points and the subsequent formation of a major X point in the tail as driven by dayside reconnection, without describing electrons in detail. This allows drawing conclusions on the overall Vlasiator physics. Our results indicate that reconnection may be a ubiquitous process within the near-Earth plasma sheet, and it may not be uncommon to have many X points operating simultaneously, interacting with each other.

Vlasiator does not use a scaled dipole strength, allowing a direct comparison of the results with the observed Earth's magnetospheric scales. We find that the first major X point builds up near the Earth at the transition region, while the last begins further away and spreads quickly along a highly elongated thin current sheet. Sergeev et al. (2012) review the current understanding of the observational location of the major X point, which can reside as close as 12 R_E in the tail to $\sim$18 R_E, agreeing well with our results. However, we note that any given X point cannot straightforwardly be mapped to the ground to be associated with observations there because several X points may operate between the observer and the ionosphere. Since the simulation is still 2-D at the moment, our results concern reconnection in a single meridional plane and cannot be generalised to concern multiple reconnection sites on a global 3-D current layer. Using a much coarser resolution, Lin et al. (2014) found multiple X lines but that dominant X lines can form if they are not competing with other X lines on a similar meridional plane. Future versions of Vlasiator shall investigate whether this is also true in the hybrid-Vlasov approach.

We also find that dayside reconnection may have direct consequences in tail reconnection, as a filled flux tube reaching the plasma sheet stabilises tail reconnection and leads to a configuration change and release of a plasmoid. The influence of density variations on the reconnection rate has been discussed in the dayside reconnection context (e.g. Wang et al., 2015; Hoilijoki et al., 2017), while on the nightside reconnection rate variations have been mostly associated with heavier ions (e.g. Liu et al., 2013). Using a 2-D MHD simulation, Hesse et al. (1996) show that the burstiness of reconnection is reduced with increasing lobe density. Here we show how these individual findings come together in the realistic magnetotail, and we predict that lobe density variations with whatever origin may influence tail reconnection condi-

tions and consequences and hence affect the overall magnetospheric dynamics as well.

Data availability. Vlasiator is distributed via http://github.com/fmihpc/vlasiator. This address contains links to the analysator software used to produce the figures. The run described here takes several terabytes of disk space and is stored within the CSC–IT Center for Science in practice. Vlasiator uses a data structure developed in-house (.vlsv format), which is compatible with the VisIt visualisation software (https://wci.llnl.gov/simulation/computer-codes/visit) with a plugin available at the above address.

The Supplement related to this article is available online at https://doi.org/10.5194/angeo-35-1269-2017-supplement.

Competing interests. The authors declare that they have no conflict of interest.

Acknowledgements. We acknowledge The European Research Council for Starting grant 200141-QuESpace, with which Vlasiator (http://vlasiator.fmi.fi) was developed, and Consolidator grant 682068-PRESTISSIMO awarded to further develop Vlasiator and use it for scientific investigations. We also gratefully acknowledge the Academy of Finland (grant numbers 267144, 267186 and 309937). PRACE (http://www.prace-ri.eu) is acknowledged for granting us Tier-0 computing time in HLRS Stuttgart, where Vlasiator was run in the HazelHen machine with project number 2014112573. The CSC – IT Center for Science in Finland is acknowledged for the sisu.csc.fi pilot usage and Grand Challenge award leading to the results presented here.

The topical editor, Christopher Mouikis, thanks two anonymous referees for help in evaluating this paper.

References

Daldorff, L. K. S., Tóth, G., Gombosi, T. I., Lapenta, G., Amaya, J., Markidis, S., and Brackbill, J. U.: Two-way coupling of a global hall magnetohydrodynamics model with a local implicit particle-in-cell model, J. Comput. Phys., 268, 236–254, https://doi.org/10.1016/j.jcp.2014.03.009, 2014.

Dungey, J. W.: Interplanetary magnetic field and the auroral zones, Phys. Rev. Lett., 6, 47–48, 1961.

Eastwood, J. P., Sibeck, D. G., Slavin, J. A., Goldstein, M. L., Lavraud, B., Sitnov, M., Imber, S., Balogh, A., Lucek, E. A., and Dandouras, I.: Observations of multiple X-line structure in the Earth's magnetotail current sheet: A Cluster case study, Geophys. Res. Lett., 32, L11105, https://doi.org/10.1029/2005GL022509, 2005.

Eastwood, J. P., Phan, T. D., Øieroset, M., and Shay, M. A.: Average properties of the magnetic reconnection ion diffusion region in the Earth's magnetotail: The 2001–2005 Cluster observations and comparison with simulations, J. Geophys. Res., 115, A08215, https://doi.org/10.1029/2009JA014962, 2010.

Hesse, M., Birn, J., Baker, D. N., and Slavin, J. A.: MHD simulations of the transition of magnetic reconnection from closed to open field lines, J. Geophys. Res., 101, 10805–10816, https://doi.org/10.1029/95JA02857, 1996.

Hoilijoki, S., Ganse, U., Pfau-Kempf, Y., Cassak, P., Walsh, B. M., Hietala, H., von Alfthan, S., and Palmroth, M.: Reconnection rates and X-line motion at the magnetopause: Global 2D-3V hybrid-Vlasov simulation results, J. Geophys. Res., 122, 2877–2888, https://doi.org/10.1002/2016JA023709, 2017.

Laitinen, T. V., Pulkkinen, T. I., Palmroth, M., Janhunen, P., and Koskinen, H. E. J.: The magnetotail reconnection region in a global MHD simulation, Ann. Geophys., 23, 3753–3764, https://doi.org/10.5194/angeo-23-3753-2005, 2005.

Lapenta, G., Markidis, S., Goldman, M., and Newman, D.: Secondary reconnection sites in reconnection- generated flux ropes and reconnection fronts, Nat. Phys., 11, 690–695, https://doi.org/10.1038/nphys3406, 2015.

Lin, Y., Wang, X. Y., Lu, S., Perez, J. D., and Lu, Q.: Investigation of storm time magnetotail and ion injection using three-dimensional global hybrid simulation, J. Geophys. Res.-Space, 119, 7413–7432, https://doi.org/10.1002/2014JA020005, 2014.

Lin, Y., Wing, S., Johnson, J. R., Wang, X. Y., Perez, J. D., and Cheng, L.: Formation and transport of entropy structures in the magnetotail simulated with a 3-D global hybrid code, Geophys. Res. Lett., 44, 5892–5899, https://doi.org/10.1002/2017GL073957, 2017.

Lyon, J. G., Brecht, S. H., Huba, J. D., Fedder, J. A., and Palmadesso, P. J.: Computer simulation of a geomagnetic substorm, Phys. Rev. Lett., 46, 1038–1041, 1981.

Lu, S., Lu, Q., Lin, Y., Wang, X., Ge, Y., Wang, R., Zhou, M., Fu, H., Huang, C., Wu, M., and Wang, S.: Dipolarization fronts as earthward propagating flux ropes: A three-dimensional global hybrid simulation, J. Geophys. Res.-Space, 120, 6286–6300, https://doi.org/10.1002/2015JA021213, 2015.

Liu, Y., Kistler, L. M., Mouikis, C. G., Klecker, B., and Dandouras, I.: Heavy ion effects on substorm loading and unloading in the Earth's magnetotail, J. Geophys. Res., 118, 2101–2112, https://doi.org/10.1002/jgra.50240, 2013.

Ohtani, S.-I., Shay, M., and Mukai, T.: Temporal structure of the fast convective flow in the plasma sheet: Comparison between observations and two-fluid simulations, J. Geophys. Res., 109, A03210, https://doi.org/10.1029/2003JA010002, 2004.

Palmroth, M., Laitinen, T. V., and Pulkkinen, T. I.: Magnetopause energy and mass transfer: results from a global MHD simulation, Ann. Geophys., 24, 3467–3480, https://doi.org/10.5194/angeo-24-3467-2006, 2006.

Palmroth, M., Honkonen, I., Sandroos, A., Kempf, Y., von Alfthan, S., and Pokhotelov, D.: Preliminary testing of global hybrid-Vlasov simulation: Magnetosheath and cusps under northward interplanetary magnetic field, J. Atom. Solar-Terr. Phy., 99, 41–46, https://doi.org/10.1016/j.jastp.2012.09.013, 2013.

Palmroth, M., Archer, M., Vainio, R., Hietala, H., Pfau-Kempf, Y., Hoilijoki, S., Hannuksela, O., Ganse, U., Sandroos, A., von Alfthan, S., and Eastwood, J.: ULF foreshock under radial IMF: THEMIS observations and global kinetic simulation Vlasiator results compared, J. Geophys. Res., 120, 8782–8798, https://doi.org/10.1002/2015JA021526, 2015.

Pulkkinen, T. I., Palmroth, M., Koskinen, H. E. J., Laitinen, T. V., Goodrich, C. C., Merkin, V. G., and Lyon, J. G.: Magnetospheric

modes and solar wind energy coupling efficiency, J. Geophys. Res., 115, A03207, https://doi.org/10.1029/2009JA014737, 2010.

Sergeev, V. A., Angelopoulos, V., and Nakamura, R.: Recent advances in understanding substorm dynamics, Geopys. Res. Lett., 39, L05101, https://doi.org/10.1029/2012GL050859, 2012.

von Alfthan, S., Pokhotelov, D., Kempf, Y., Hoilijoki, S., Honkonen, I., Sandroos, A., and Palmroth, M.: Vlasiator: First kinetic global hybrid-Vlasov simulation code for modelling space plasma, J. Atmos. Solar-Terr. Phy., 120, 24–35, https://doi.org/10.1016/jjastp.2014.08.012, 2014.

Wang, S., Kistler, L. M., Mouikis, C. G., and Petrinec, S. M.: Dependence of the dayside magnetopause reconnection rate on local conditions, J. Geophys. Res.-Space, 120, 6386–6408, https://doi.org/10.1002/2015JA021524, 2015.

Watermann, J., Wintoft, P., Sanahuja, B., Saiz, E., Poedts, S., Palmroth, M., Milillo, A., Metallinou, F.-A., Jacobs, C., Ganushkina, N. Y., Daglis, I. A., Cid, C., Cerrato, Y., Balasis, G., Aylward, A. D., and Aran, A.: Models of Solar Wind Structures and Their Interaction with the Earth's Space Environment, Space Sci. Rev., 147, 233–270, https://doi.org/10.1007/s11214-009-9494-9, 2009.

Wiltberger, M., Merkin, V., Lyon, J. G., and Ohtani, S.: High-resolution global magnetohydrodynamic simulation of bursty bulk flows, J. Geophys. Res., 120, 4555–4566, https://doi.org/10.1002/2015JA021080, 2015.

Yeates, A. R. and Hornig, G.: A generalized flux function for three-dimensional magnetic reconnection, Phys. Plasmas, 18, 102118, https://doi.org/10.1063/1.3657424, 2011.

Zeiler, A., Biskamp, D., Drake, J. F., Rogers, B. N., Shay, M. A., and Scholer, M.: Three-dimensional particle simulations of collisionless magnetic reconnection, J. Geophys. Res., 107, 9 pp., https://doi.org/10.1029/2001JA000287, 2002.